NUMERICAL STUDY ON NUSSELT NUMBER OF MOVING PHASE INTERFACE DURING WAX MELTING IN TUBE USING LATTICE BOLTZMANN METHOD

by

Zheng ZHOU[a], Xiao-Yan LIU[a], Xiao-Qing LI[b], Ying XU[a], and Zhi-Zhuang WANG[a]*

[a] School of Civil and Engineering, Northeast Petroleum University, Daqing, China
[b] School of Electronic and Information Engineering,
Changshu Institute of Technology, Changshu, China

Paraffin melting is widely applied to the fields of PCM energy storage, gathering and transportation pipe-line paraffin removal, etc. Natural-convection is the main heat transfer mode during paraffin melting, and Rayleigh number is an important factor affecting the change of natural-convection intensity. Nusselt number variation can reflect the influence of natural-convection on heat transfer. The conventional Nusselt number of hot wall surface reflects only the convective heat transfer intensity of the fixed wall, while it does not take into account that the phase change interface has the characteristics of moving in the phase change process. A double distribution model of paraffin phase transformation in circular tube based on lattice Boltzmann method is established in this paper. The influence of Rayleigh number on the temperature field and flow field of wax in circular tube is analyzed. The heat transfer process is reflected by Nusselt number of moving phase interface. The relation between Nusselt number of moving interface and Nusselt number of hot wall surface is also presented. The results show that the Nusselt number of moving phase interface can reflect the complex non-linear characteristics of natural-convection and describe the phase change heat transfer process of wax more accurately. Calculation formula of Nusselt number of moving phase interface and hot wall during wax phase change is proposed. Increasing Rayleigh number can quicken the melting of wax to meet the actual engineering requirements.

Key words: *thermal washing for the waxy deposition, lattice Boltzmann method, Rayleigh number, Nusselt number of mobile phase interface*

Introduction

Wax is an important part of crude-oil. Crude-oil will continuously precipitate paraffin crystals during the pipe-line transportation, resulting in paraffin deposition in the pipe-line and affecting the transportation safety of the gathering pipe-line [1-3]. Thermal washing for the waxy deposition is used widely in gathering and transportation pipe-lines [4]. Xu *et al.* [5] proposed a new wide phase change partition model. The phase change heat transfer process was analyzed by using the trajectory of the highest temperature, and the influence of natural-convection heat transfer process of shutdown crude-oil were discussed. Yu *et al.* [6, 7] reported a phase change heat transfer model suitable for waxy crude-oil. The heat transfer process of

---

4958

Zhou, Z., *et al.*: Numerical Study on Nusselt Number of Moving Phase ...
THERMAL SCIENCE: Year 2022, Vol. 26, No. 6B, pp. 4957-4967

waxy crude-oil after shutdown was studied and the cooling wax precipitation characteristics of crude-oil was clarified. Jiang *et al*. [8] used CFD method to simulate the melting process of waxy deposition in gathering pipe-line, and the influence of water temperature and flow rate on waxy deposition removal efficiency was studied. Li *et al*. [9] studied the melting and flow characteristics of waxy deposition in gathering pipe-line by CFD method. The relational expression for predicting the complete melting time of wax in natural-convection was proposed to guide the thermal washing for the waxy deposition.

It can be seen that the phase change process of crude-oil is complex, and there are few studies on the thermal washing for the waxy deposition from the wax melting mechanism. The simulation method of pipe-line thermal washing for the waxy deposition is mainly CFD method. The process of thermal washing for the waxy deposition is actually a phase change heat transfer process of wax in the pipe-line, which involves complex solid-liquid phase change process. Conventional CFD methods have great limitations in complex structures mesh generation, boundary treatment and solid-liquid interface tracking. Lattice Boltzmann method (LBM) is used widely in the field of multi-phase flow and solid-liquid phase change due to its mesoscopic physical background. The research on heat transfer process using LBM mainly focuses on energy storage and fluid heat transfer. Research on such problems provides a reference for this paper.

Li *et al.* [10] and Zhang *et al.* [11] studied the melting of PCM in square cavity by LBM. Feng *et al.* [12] studied the phase change process of particle reinforced phase change materials in the bottom heating square cavity by LBM. The change of Nusselt number on the hot wall was analyzed, and it was considered that the particles promoted the melting process. Lin *et al.* [13] utilized LBM to study the melting problem of PCM in spheres with different sizes. The correctness of the axisymmetric enthalpy model was verified Nusselt number on the hot wall. Lu *et al.* [14] utilized LBM to study the electrothermal melting of concentric annular PCM. The convective heat transfer process was analyzed through the change of Nusselt number on the hot wall. Rao *et al.* [15] and Mahmoud and Morteza [16] also studied the effects of cavity tilt angle on Nusselt number on hot wall and convective heat transfer coefficient. Yao *et al.* [17] utilized LBM to study the heat transfer process of paraffin in square cavity with obstacles. The phase change process is divided into four stages according to the variation of Nusselt number on the hot wall with time. Yao *et al.* [18] utilized LBM to simulate the natural-convection in a square cavity partially filled with porous media. Natural-convection is analyzed by the change of Nusselt number on hot wall. Zhao *et al.* [19] studied the forced convection heat transfer of nanofluids in porous channels using LBM. It is considered that the addition of nanoparticles significantly increases the Nusselt number on hot wall. Gangawane *et al.* [20] studied the heat transfer process of fluid in the square cover drive cavity with triangular blocks, and the empirical formula for Nusselt number calculation about dimensionless length, triangular block position and Rayleigh number were proposed. Hasnaoui *et al.* [21] utilized LBM to study the natural-convection heat transfer process in the square cavity with Soret effect and internal heat source, and analyzed the simulation results by the change of Nusselt number on the hot wall. Ibrahim *et al.* [22, 23] utilized LBM to study the natural convective heat transfer process of nanofluids in an inner heat source square cavity and a quarter of a circular tube, selected the relevant parameters of the highest heat transfer rate through the optimization of neural network algorithm. Mohebbi *et al.* [24] utilized LBM to study the influence of Rayleigh number in nanofluids square cavities with different roughness on Nusselt number of hot wall. Sajjadi and Kefayati [25] studied the natural-convection of fluid in rectangular cavity under high Rayleigh number. The effects of different Rayleigh numbers and rectangular aspect ratios on the Nusselt number of hot wall were explored.

Zhou, Z., *et al.*: Numerical Study on Nusselt Number of Moving Phase ...
THERMAL SCIENCE: Year 2022, Vol. 26, No. 6B, pp. 4957-4967

4959

The heat transfer problems of rectangular cavity, cylindrical cavity and spherical cavity have been extensively studied in summary. These PCM do not have wide phase transition temperature region. The Nusselt number of the hot wall can only reflect the convective intensity between the fixed wall and the liquid wax. However, the position of the solid-liquid interface is constantly changing inward due to the continuous melting of wax in practical engineering, and the position of natural convective heat transfer with solid wax is also changing. Therefore, the moving phase interface Nusselt number can accurately describe the convective heat transfer intensity at the wax phase change position. A 2-D lattice Boltzmann model based on enthalpy was established to simulate the wax melting process in a 2-D cylindrical cavity in this paper. The effect of different Rayleigh numbers on wax phase change process were studied. The change of Nusselt number on the moving phase interface was calculated to describe the natural-convection process of wax. The calculation formula between Nusselt number of hot wall and Nusselt number of moving phase interface is presented. This paper can provide some guidance for the pipe-line thermal washing for the waxy deposition.

Method and materials

Physical model

Figure 1 is the wax melting diagram of 2-D cylindrical cross-section. Assuming that the cylindrical cavity is filled with uniformly distributed wax, and the axial heat transfer of the pipe-line is ignored. The initial temperature of wax is T_1, and the wall temperature is T_w, $T_w > T_1$. The T_s and T_1 are the temperatures at the beginning of melting and at the end of melting. As the heat transfer progresses, the wax is in the solid zone when the temperature is lower than T_s, and the heat transfer mode is heat conduction. No phase change occurred in wax at this time. The phase change temperature of wax is a large temperature range. The wax begins to change phase when the temperature rises between T_s and T_1. The wax in the

Figure 1. The 2-D cylindrical cross-section wax melting diagram

fuzzy zone is in a solid-liquid mixing zone, and the heat transfer mode is heat conduction and heat convection. The wax completely becomes liquid when the temperature is higher than T_1, and the heat transfer mode is thermal convection.
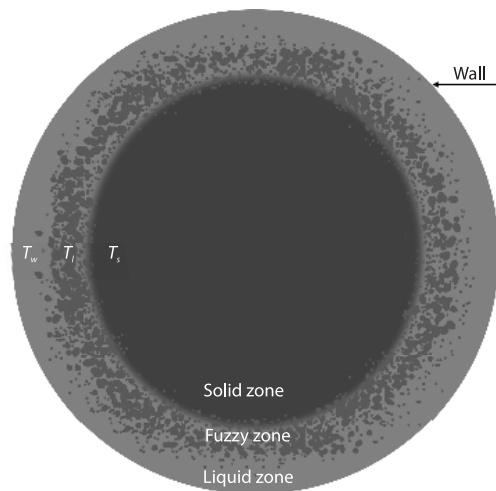
Mathematical model

Considering the non-linear characteristics of transient melting and the complexity of wax composition, the mathematical model of wax phase transformation heat transfer is based on the boussinesq assumption, and the fuzzy zone is simplified as a multi-phase flow zone.

Governing equations

$$\nabla \vec{u} = 0 \tag{1}$$

$$\frac{\partial \vec{u}}{\partial t} + (\vec{u}\nabla)\vec{u} = -\nabla p + = \nu\nabla^2\vec{u} - g\beta(T - T_m) \tag{2}$$

$$\frac{\partial T}{\partial t} + \vec{u}\nabla T = \alpha\nabla^2 T - \frac{L_a}{C_l}\frac{\partial f_l}{\partial t} \tag{3}$$

Equation (1) is the continuity equation. Equation (2) is the momentum equation, and the pressure, viscous stress and buoyancy of wax are considered on the right side of the momentum equation. Equation (3) is the energy equation.

Parameters u, T, and p are the velocity, temperature, and pressure of the fluid and v, C_l, and L_a are the kinematic viscosity, specific heat capacity under constant pressure, and latent heat of phase change while β, α, and f_l are the volume expansion coefficient, thermal diffusion coefficient, and liquid ratio.

Temperature and liquid ratio are mutually coupled, so the enthalpy method is used to calculate the liquid ratio [26]:

$$H_p = C_l T + f_l L_a \tag{4}$$

$$f_l = \frac{H_p - H_{ps}}{H_{pl} - H_{ps}} \tag{5}$$

Lattice Boltzmann model

The density distribution function is used to describe the velocity field and the temperature distribution function is used to describe the temperature field in this paper. Density distribution function evolution equation using Bhatnager-Gross-Krook approximate double distribution function model based on Boussinesq assumption proposed by Guo [27]:

$$+ e_i\Delta t, t+\Delta t) - f_i(r,t) = -\frac{1}{\tau_f}\left[f_i(r,t) - f_i^{eq}(r,t)\right] + \Delta t F_i \tag{6}$$

$$f_i^{eq} = \omega_i\rho\left[1 + 3\frac{e_i u}{c^2} + 4.5\frac{(e_i u)^2}{c^4} - 1.5\frac{u^2}{c^2}\right] \tag{7}$$

$$F_i = \left(1 - \frac{1}{2\tau_f}\right)\omega_i\left[3\frac{e_i - u}{c^2} + 9\frac{e_i u}{c^4}e_i\right]\left[\beta g(T - T_m)\right] \tag{8}$$

where f_i and f_i^{eq} are the density distribution function and density equilibrium distribution function, r – the space vector position, e_i – the lattice discrete velocity, t – the time, Δt – the unit time step, τ_f – the dimensionless relaxation time of density distribution function, F_i – the force, ω_i – the weight coefficient, u – the velocity, $c = \Delta x/\Delta t$ – the lattice velocity, ρ – the density, and Δx – the lattice step size.

There is a non-linear source term in the heat transfer equation of wax melting. Therefore, the lattice Boltzmann model of non-linear convection diffusion equation proposed by Shi and Guo [28] is used as the evolution equation of temperature distribution function:

$$g_i(r + e_i\Delta t, t+\Delta t) - g_i(r,t) = -\frac{1}{\tau_T}\left[g_i(r,t) - g_i^{eq}(r,t)\right] + \Delta t S_i \tag{9}$$

$$g_i^{eq} = \omega_i T\left[1 + 3\frac{e_i u}{c^2} + 4.5\frac{(e_i u)^2}{c^4} - 1.5\frac{u^2}{c^2}\right] \tag{10}$$

$$S_i = -\omega_i\frac{L_a}{C_l}\frac{f_l(t+\Delta t) - f_l(t)}{\Delta t}\left[1 + \left(1 - \frac{1}{2\tau_T}\right)\frac{3e_i u}{c^2}\right] \tag{11}$$

Zhou, Z., *et al.*: Numerical Study on Nusselt Number of Moving Phase ...
THERMAL SCIENCE: Year 2022, Vol. 26, No. 6B, pp. 4957-4967

4961

where g_i and g_i^{eq} are the temperature distribution function and temperature equilibrium distribution function, τ_T – the dimensionless relaxation time of temperature distribution function, T – the temperature, and S_i – the non-linear source term.

The dimensionless relaxation time of density distribution function and temperature distribution function are:

$$\tau_f = \frac{3\nu}{c^2 \Delta t} + 0.5 \qquad (12)$$

$$\tau_T = \frac{3\alpha}{c^2 \Delta t} + 0.5 \qquad (13)$$

Variable relaxation time is used to study variable thermophysical properties. For ease of calculation, the relaxation time is controlled between (0.5, 2) [29]. The relaxation time of the temperature distribution function evolution equation in the fuzzy zone is expressed by Jiaung *et al.* [26]:

$$\tau = \frac{1}{2} + \frac{\alpha_l}{\alpha_s}\left(\tau_s - \frac{1}{2}\right)f_l \qquad (14)$$

where α_l and α_s are the thermal diffusion coefficients of liquid and solid and τ_s is the dimensionless relaxation time of the evolution equation of solid wax temperature distribution function.

Macroscopic density and velocity calculations:

$$\rho = \sum_i f_i, \ u = \frac{\sum_i e_i f_i}{\rho} + \frac{\vec{F}\Delta t}{2} \qquad (15)$$

Equations (6) and (9) can be regressed to the control equations through Chapman-Enskog expansion.

Model validation

The visualization experiment of wax melting in the tube was carried out in this paper. The inner diameter of the tube is 61 mm. The initial temperature of wax is 21 °C, and the outer wall of the tube is heated by heating band at 52 °C. The related physical parameters of wax are measured by TPS2200 thermal constant analyzer as the basic parameters of numerical calculation. Detailed parameters are shown in tab. 1.

Figure 2 is the phase diagram comparison between the visualization experiment and the simulation results when Fo = 0.0473. It can be seen from the diagram that the melting mor-

Table 1. Physical parameters of wax

Physical parameters		Numerical value
Density	Liquid phase	890.75 kg/m³
	Solid phase	932.06 kg/m³
Specific heat capacity	Liquid phase	3054 J/kg°C
	Solid phase	1797 J/kg°C
Thermal conductivity	Liquid phase	0.18 W/m°C
	Solid phase	0.23 W/m°C
Kinematic viscosity		5.94 mPa·s
Latent heat		185.88 kJ/kg
Phase transition temperature region		40.0-61.0 °C
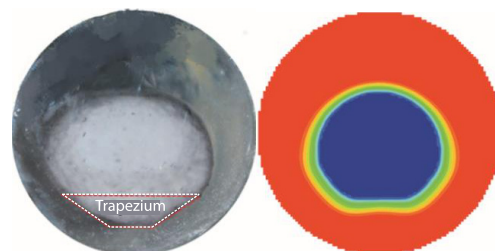
Figure 2. Visualization experiment and simulation phase diagram (Fo = 0.0473)

4962

Zhou, Z., *et al.*: Numerical Study on Nusselt Number of Moving Phase ...
THERMAL SCIENCE: Year 2022, Vol. 26, No. 6B, pp. 4957-4967

phomogy of wax is similar, and the bottom of solid wax has an approximate trapezoidal shape. The liquid ratios measured by visualization experiment is 69.39%. The liquid ratios measured by simulation is 73.15%. The relative error is 5.4%. The liquid ratios of visualization experiments and simulations with different Fourier numbers are measured and the errors are calculated. The results are shown in tab. 2.

Table 2. Liquid ratio error between visualization experiment and simulation

Fo	Liquid ratio of visualization experiment [%]	Liquid ratio of numerical calculation [%]	Relative error [%]
0	0.00	0.00	0
0.0209	37.43	40.31	7.41
0.0225	41.26	43.81	6.18
0.0376	62.08	63.42	2.16
0.0532	75.48	81.26	7.65
0.0602	83.98	91.25	8.65

Due to the the fuzzy zone in the simulation is assumed a multi-phase flow zone, the influence of the porous medium region is ignored, resulting in faster heat transfer rate. Thus the simulated liquid ratio is higher than the experimental one. Our hypothesis is based on the ideal state of heat transfer. In addition, the wide temperature range of the fuzzy zone and temperature control of the heating zone also cause some errors. It can be seen from tab. 2. that the maximum relative error, minimum relative error and average relative error of liquid ratios obtained by visual experiment and numerical simulation are 8.65%, 2.16%, and 6.41 %, which meets the requirements of engineering accuracy.

Result and discussion

Effect of Rayleigh number on flow field and temperature field

The change of wax temperature field under different Rayleigh number is shown in fig. 3. The change of wax flow field under different Rayleigh number is shown in fig. 4. It can be seen from fig. 3 that the wax in the cylinder is melted by heating, and a thin layer of fuzzy zone appears between the wax and the wall at the initial phase of heat transfer. The overall wax temperature field has a concentric circular distribution. This is due to shown in fig. 4 that the wax flow field is distributed along the wall and the shape is regular. Since most of the solid wax is in the cylinder this time, the effect of natural-convection on heat transfer is not obvious and heat conduction is the main way of heat transfer. Liquid wax gradually increased, and the fuzzy zone continued to thicken in the middle of heat transfer. The temperature field shows an irregular ellipse. This change is more obvious with the Rayleigh number increasing. This is due to shown in fig. 4 that the area of liquid wax in the upper half of the tube increases during the mid-term heat transfer. Liquid wax rises along the tube wall under the action of buoyancy, and then sinks from the center of the tube, resulting in natural-convection enhance the heat transfer ability. The natural-convection intensity increases gradually with the Rayleigh number increasing. Most of the tube is liquid wax in the later stage of heat transfer, the temperature field distribution is more irregular, and the convective heat transfer intensity continues to increase. Figure 3 shows that the temperature field distribution is more irregular. Figure 4 tells that small local vortices appear at the bottom of the pipe when Ra = $1.0 \cdot 10^6$. This is due to the increase of Rayleigh number makes the natural-convection intensity increase, and the increase of the intensity will cause local vortex in a smaller space. In addition, convective heat transfer has complex non-linear characteristics, which will lead to uneven distribution of flow field.
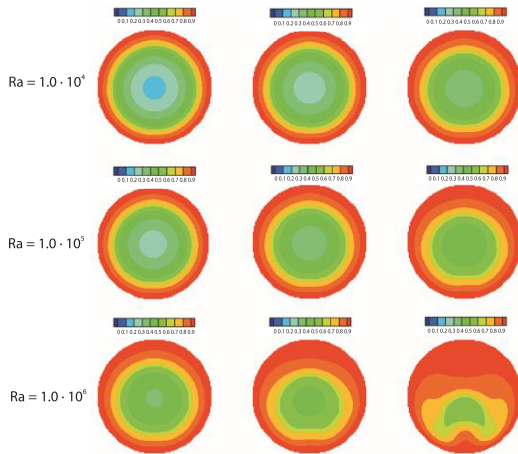
Figure 3. Temperature field changes of wax under different Rayleigh numbers; (a) Fo = 0.0285, (b) Fo = 0.0350, and (c) Fo = 0.0430
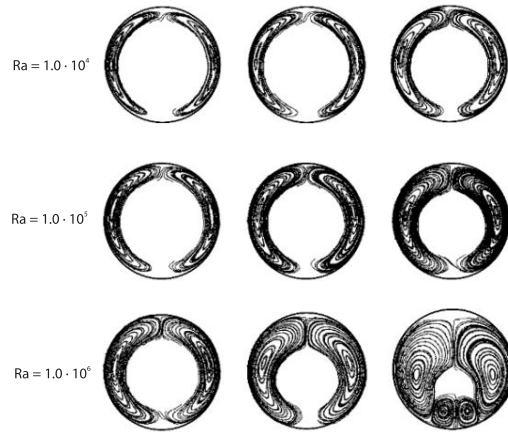

Figure 4. Flow field changes of wax under different Rayleigh numbers; (a) Fo = 0.0285, (b) Fo = 0.0350, and (c) Fo = 0.0430

Effect of Rayleigh number on Nusselt number

Nusselt number of the hot wall was usually utilized to analyze and evaluate the heat transfer process in the past. The phase interface between liquid wax and solid wax gradually moves in the melting process, and thus the Nusselt number of the hot wall cannot accurately describe the convective heat transfer between the phase interface. Therefore, this paper uses the Nusselt number of the mobile phase interface to analyze the wax phase transformation process in the pipe wall.

The change of Nu_i with Fourier number under different Rayleigh numbers is shown in fig. 5. The Nu_i is Nusselt number of mobile phase interface. It can be seen from fig. 5 that Nu_i decreased close to zero during the whole melting process. The Nu_i curves under different Rayleigh numbers almost coincide in the initial phase of heat transfer. Liquid wax accounts for a small proportion in this phase of heat transfer, and the main heat transfer mode is heat conduction in the solid zone. Since the natural-convection has not yet become dominant, the change of Rayleigh number has little effect on the change of Nu_i. The decrease rate of Nu_i is significantly accelerated when Rayleigh number increased from $1.0 \cdot 10^4$ to $1.0 \cdot 10^5$, and $1.0 \cdot 10^6$. The reason is that natu-

ral-convection dominates heat transfer, and the intensity of natural-convection increases with the increase of Rayleigh number. The shape of Nu_i change curve is almost the same when $Ra = 1.0 \cdot 10^5$ and $Ra = 1.0 \cdot 10^6$. This is due to shown in fig. 4 that a large Rayleigh number will form multiple local vortices in the liquid zone. Although increasing Rayleigh number will increase the intensity of natural-convection, the existence of local vortices will inhibit the heat and mass transfer. Therefore, the Nu_i variation curve is almost coincident when
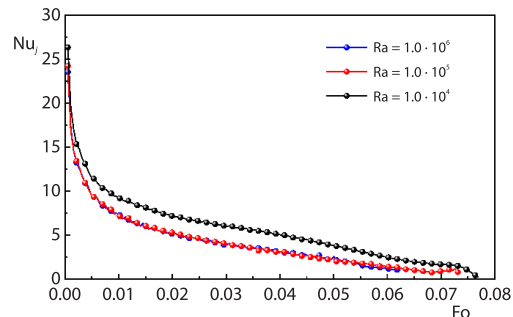

Figure 5. The Nu_i change under different Rayleigh numbers

4964

Zhou, Z., *et al.*: Numerical Study on Nusselt Number of Moving Phase ...
THERMAL SCIENCE: Year 2022, Vol. 26, No. 6B, pp. 4957-4967

$Ra = 1.0 \cdot 10^5$ and $Ra = 1.0 \cdot 10^6$. The Nu_i oscillates with the increase of Rayleigh number in the middle and later phase of heat transfer. Since the convective heat transfer is non-linear and occurs at the mobile phase interface, resulting in fluctuations of temperature gradient and makes the Nu_i to oscillate.

Correction of Nusselt number

According to the aforementioned analysis, the heat transfer process analysis using Nusselt number of phase interfaces is more accurate. The relationship between the Nusselt number of the hot wall and the Nusselt number of the moving phase interface under different Rayleigh numbers obtained by numerical simulation is shown in fig. 6. The Nusselt number of the phase interface is Nu_i and the Nusselt number of the hot wall is Nu_w.

The curves of two kinds of Nusselt number under different Rayleigh numbers are similar is shown in fig. 6, but numerical oscillation occurs in the middle of heat transfer. This is due to the medium-term heat transfer involves the change of heat transfer mode from heat conduction natural-convection. Natural-convection has complex non-linear characteristics, and it will produce local vortices which are difficult to observe at the interface, so that the temperature gradient at the moving phase interface fluctuates resulting in oscillation.
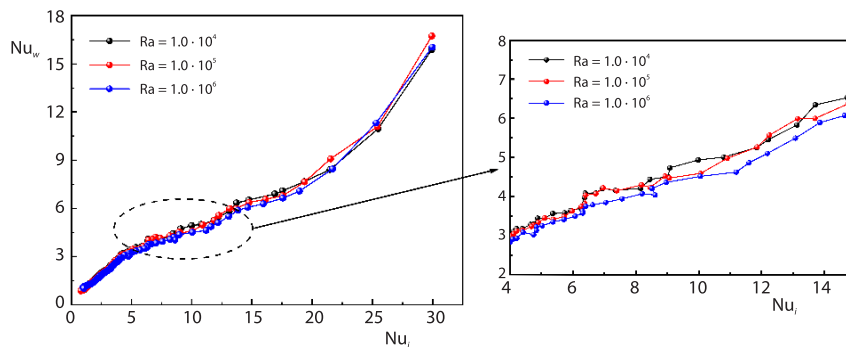

Figure 6. Variation relationship and local amplification diagram of two types of Nusselt numbers under different Rayleigh numbers

Figure 7 shows the fitting curves of the relationship between the Nu_i and the Nu_w under different Rayleigh numbers. The result shows that the relationship between Nu_i and Nu_w satisfies the cubic function under different low Rayleigh numbers. The following fitting relationship is obtained by weighted average:

$$Nu_w = 0.15613 + 0.81616 Nu_i - 0.04647 Nu_i^2 + 0.00124 Nu_i^3 \qquad (16)$$

The Nusselt number of the hot wall is recalculated by eq. (16), and compare with the simulation results to verify the correctness of the relationship. The specific error is shown in tab. 3.

Table 3 tells that the minimum error is 0.51%, the maximum error is 3.45%, and the average error is 1.69% when $Ra = 1.0 \cdot 10^4$. The minimum error is 0.54%, the maximum error is 3.64%, and the average error is 1.80% when $Ra = 1.0 \cdot 10^5$. The minimum error is 0.65%, the maximum error is 4.95 %, and the average error is 3.90 % when $Ra = 1.0 \cdot 10^6$. The error is less than 5.00%, which meets the engineering accuracy requirements. Two types of Nusselt number relations under different low Rayleigh numbers are correct.
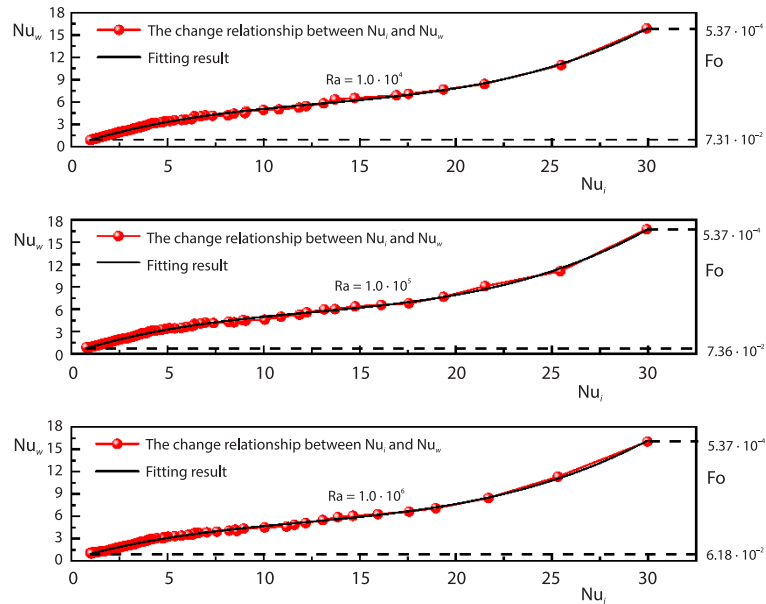
Figure 7. Variation relationship and fitting curve of Nu_i and Nu_w under different Rayleigh numbers

Table 3. Error comparison between simulation and formula

Nu_w (Ra = $1.0 \cdot 10^4$)		Error [%]	Nu_w (Ra = ($1.0 \cdot 10^5$)		Error [%]	Nu_w (Ra = $1.0 \cdot 10^6$)		Error [%]
Simulation	Formula		Simulation	Formula		Simulation	Formula	
7.09	6.85	−3.45	6.79	6.85	−0.91	6.63	6.85	−3.34
2.23	2.22	−0.51	2.22	2.23	−0.54	3.84	4.03	−4.95
2.13	2.11	−1.08	2.08	2.11	−1.54	2.03	2.11	−4.35
1.19	1.21	1.11	1.17	1.21	−3.64	1.60	1.67	−4.37
1.07	1.08	1.59	1.05	1.09	−3.40	1.27	1.26	0.65
0.96	0.98	2.42	0.94	0.95	−0.78	1.17	1.12	4.54

Conclusions

- The influence of the Rayleigh number on heat transfer process is not obvious in the initial phase of wax melting. The influence of Rayleigh number is gradually increased with the increases of Fourier number. The temperature field appears irregular in shape, and the flow field appears as a local vortex when Rayleigh number increases from $1.0 \cdot 10^4$ to $1.0 \cdot 10^6$. The melting rate increases until the wax is completely melted when Rayleigh number increases from $1.0 \cdot 10^4$ to $1.0 \cdot 10^6$.

- Rayleigh number had no significant effect on Nusselt number in the initial phase of heat transfer. The decrease rate of Nusselt number is significantly enhanced when the Rayleigh number increases from $1.0 \cdot 10^4$ to $1.0 \cdot 10^6$ in the middle and late phases of heat transfer. The increase of natural-convection intensity will lead to temperature mutation at the phase interface in the late phase of heat transfer. The heat transfer process can be described more clearly and accurately by Nu_i.

- The change of heat transfer mode will lead to the fluctuation of temperature gradient at the moving phase interface in the middle of heat transfer. The relation between Nu_i and Nu_w under different low Rayleigh number is proposed.
- The wax melting rate increases and melting time shorten when Rayleigh increases from $1.0 \cdot 10^4$ to $1.0 \cdot 10^6$. Therefore, the wax removal rate can be improved by increasing the Rayleigh number in practical engineering.

Acknowledgment

Nomenclature

C_l – specific heat capacity at constant pressure
c – lattice speed, [ms^{-1}]
e_i – microscopic particle velocity in each lattice
F – external force, [N]
f_l – liquid fraction
g – distribution function for temperature
H_p – enthalpy
L_a – latent heat of melting
Nu – Nusselt number
Ra – Rayleigh number
S – source term
T – macroscopic temperature, [K]
t – time, [s]

Δt – time step
u – velocity in the x-direction, [ms^{-1}]

Greek symbols

α – thermal diffusivity, [m^2s^{-1}]
β – thermal expansion coefficient
γ – volume fraction
v – kinematic viscosity, [m^2s^{-1}]
ρ – fluid density, [kgm^{-3}]
σ – thermal capacity ratio
τ – dimensionless relaxation time
ω – weight function

References

[1] Gan, Y., *et al.*, Molecular Dynamics Simulation of Waxy Crude-oil Multi-phase System Depositing and Sticking on Pipe-Line Inner Walls and the Micro Influence Mechanism of Surface Physical-Chemical Characteristics, *Energy and Fuels*, *35* (2021), 5, pp. 4012-4028
[2] Liu, X., *et al.*, Numerical Investigation of Waxy Crude-Oil Paste Melting on an Inner Overhead Pipe Wall, *Applied Thermal Engineering*, *131* (2018), Feb., pp. 779-785
[3] Makwashi, N., *et al.*, Study on Waxy Crudes Characterisation and Chemical Inhibitor Assessment, *Journal of Petroleum Science and Engineering*, *204* (2021), Sept., 108734
[4] Li, W., *et al.*, Advances and Future Challenges of Wax Removal in Pipe-line Pigging Operations on Crude-oil Transportation Systems, *Energy Technology*, *8* (2020), 6, 1901412
[5] Xu, Y., *et al.*, Heat Transfer Analysis of Waxy Crude-Oil under a New Wide Phase Change Partition Model, *Numerical Heat Transfer, Part A: Applications*, *76* (2019), 12, pp. 991-1005
[6] Yu, G., *et al.*, A New General Model for Phase-Change Heat Transfer of Waxy Crude-Oil during the Ambient-Induced Cooling Process, *Numerical Heat Transfer, Part A: Applications*, *71* (2017), 5, pp. 511-527
[7] Yu, G., *et al.*, Further Study on the Thermal Characteristic of a Buried Waxy Crude-Oil Pipe-Line during Its Cooling Process after a Shutdown, *Numerical Heat Transfer, Part A: Applications*, *71* (2017), 2, pp. 137-152
[8] Jiang, H., *et al.*, Numerical Study for Removing Wax Deposition by Thermal Washing for the Waxy Crude-Oil Gathering Pipe-Line, *Sci Prog*, *103* (2020), 3, 36850420958529
[9] Li, X., *et al.*, Numerical Investigation on the Melting Characteristics of Wax for the Safe and Energy-Efficiency Transportation of Crude-Oil Pipe-Lines, *Measurement: Sensors*, *10-12* (2020), Nov., 100022
[10] Li, Z., *et al.*, Numerical Simulation of Melting Problems Using the Lattice Boltzmann Method with the Interfacial Tracking Method, *Numerical Heat Transfer, Part A: Applications*, *68* (2015), 11, pp. 1175-1197
[11] Zhang, T., *et al.*, Numerical Study of Convection in Phase Change Material Based on Lattice-Boltzmann Method, IOP Conference Series: *Materials Science and Engineering*, *207* (2017), 1, 012072
[12] Feng, Y., *et al.*, Numerical Investigation on the Melting of Nanoparticle-Enhanced Phase Change Materials (NEPCM) in a Bottom-Heated Rectangular Cavity Using Lattice Boltzmann method, *International Journal of Heat and Mass Transfer*, *81* (2015), Feb., pp. 415-425

[13] Lin, Q.*, et al.*, Lattice Boltzmann Simulation of Flow and Heat Transfer Evolution Inside Encapsulated Phase Change Materials Due to Natural-Convection Melting*, Chemical Engineering Science*, *189* (2018), Nov., pp. 154-164
[14] Lu, C.-L.*, et al.*, Lattice Boltzmann Analysis for Electro-Thermo-Convection with a Melting Boundary in Horizontal Concentric Annuli*, Physics of Fluids*, *33* (2021), 4, 043605
[15] Rao, Z.*, et al.*, The Lattice Boltzmann Investigation for the Melting Process of Phase Change Material in an Inclined Cavity*, Journal of Heat Transfer*, *140* (2018), 1, 012301
[16] Ahmed, M., Eslamian, M., Numerical Simulation of Natural-Convection of a Nanofluid in an Inclined Heated Enclosure Using Two-Phase Lattice Boltzmann Method: Accurate Effects of Thermophoresis and Brownian Forces*, Nanoscale Res Lett*, *10* (2015), 1, 1006
[17] Yip, Y. H.*, et al.*, Flow-Dynamics Induced Thermal Management of Crude-Oil Wax Melting: Lattice Boltzmann Modelling*, International Journal of Thermal Sciences*, *137* (2019), Mar., pp. 675-691
[18] Yao, S. G.*, et al.*, The Study of Natural-convection Heat Transfer in a Partially Porous Cavity Based on LBM*, The Open Fuels & Energy Science Journal*, *7* (2014), 1, pp. 88-93
[19] Zhao, Q.*, et al.*, Lattice Boltzmann Method for Nanofluid Forced Convection Heat Exchange in a Porous Channel with Multiple Heated Sources*, Numerical Heat Transfer, Part A: Applications*, *79* (2020), 1, pp. 21-39
[20] Gangawane, K. M.*, et al.*, Mixed Convection in a Lid-Driven Cavity Containing Triangular Block with Constant Heat Flux: Effect of Location of Block*, International Journal of Mechanical Sciences*, *152* (2019), Mar., pp. 492-511
[21] Hasnaoui, S.*, et al.*, Hybrid Lattice Boltzmann Finite Difference Simulation of Soret Convection Flows in a Square Cavity with Internal Heat Generation*, Numerical Heat Transfer, Part A: Applications*, *74* (2018), 1, pp. 948-973
[22] Ibrahim, M.*, et al.*, Optimization and Effect of Wall Conduction on Natural-Convection in a Cavity with Constant Temperature Heat Source: Using Lattice Boltzmann Method and Neural Network Algorithm*, Journal of Thermal Analysis and Calorimetry*, *144* (2021), 6, pp. 2449-2463
[23] Ibrahim, M.*, et al.*, The Effects of L-Shaped Heat Source in a Quarter-Tube Enclosure Filled with MHD Nanofluid on Heat Transfer and Irreversibilities, Using LBM: Numerical Data, Optimization Using Neural Network Algorithm (ANN)*, Journal of Thermal Analysis and Calorimetry*, *144* (2021), 6, pp. 2435-2448
[24] Mohebbi, R.*, et al.*, Natural-Convection Heat Transfer of Nanofluid Inside a Cavity Containing Rough Elements Using Lattice Boltzmann Method*, International Journal of Numerical Methods for Heat and Fluid-Flow*, *29* (2019), 10, pp. 3659-3684
[25] Sajjadi, H., Kefayati, R., Lattice Boltzmann Simulation of Turbulent Natural-Convection in Tall Enclosures*, Thermal Science*, *19* (2015), 1, pp. 155-166
[26] Jianng, W.-S.*, et al.*, Lattice Boltzmann Method for the Heat Conduction Problem with Phase Change*, Numerical Heat Transfer, Part B: Fundamentals*, *39* (2001), 2, pp. 167-187
[27] Guo, Z.*, et al.*, A Coupled Lattice BGK Model for the Boussinesq Equations*, International Journal for Numerical Methods in Fluids*, *39* (2002), 4, pp. 325-342
[28] Shi, B., Guo, Z., Lattice Boltzmann Model for Non-Linear Convection-Diffusion Equations*, Physical Review E*, *79* (2009), 1, 016701
[29] Wang, M., Pan, N., Modelling and Prediction of the Effective Thermal Conductivity of Random Open-Cell Porous Foams*, International Journal of Heat & Mass Transfer*, *51* (2008), 5-6, pp. 1325-1331